

Invited review

Radiation track and DNA damage

H. Nikjoo*

MRC Radiation and Genome Stability Unit, Harwell, Oxfordshire, OX11 0RD, UK.

Keywords: *Track structure, DNA damage, clustered damage, energy deposition, adaptive response, bystander.*

INTRODUCTION

This article provides a brief review of aspects of biophysical modelling in radiation biology. A major concern of radiation biology in the past half century has been the quantification of the health hazards of ionising radiations of different qualities and extrapolation of human cancer risks at high dose and dose rates to low dose and dose rates (UNSCEAR 1993). In the past decade with the accelerated progress in molecular biology techniques and advances in theoretical methods attention has become more focused on mechanistic studies and interpretation of effects of ionising radiation. To this end, track structure has provided a theoretical tool to investigate those parameters of ionising radiation that predominantly determine the nature and magnitude of the final effect (Vogelstein and Kinzler 1998).

Radiation oncogenesis is a multistep process including the *initiation* stage, the *promotion* or expansion processes, the *conversion* stage and the final stage of *progression*. In the initiation stage radiation produces *molecular damage* by modification of the primary structure of DNA following the passage of the particle through the cell. The initial *molecular damage* is subject to

modification and amplification by cellular responses to maintain the genetic stability of the cell. In majority of cases the initial damage to the DNA structure is reparable depending on the physical type of damage and physiological conditions of the cell. Post modification of the molecular damage could lead to *specific biological lesions*, such as genetic instability, chromosomal aberration and mutation in a specific target somatic cell. Expression of the particular mutational event through the cell cycle initiates the colonial *expansion* of the oncogenic processes which could lead to the final stage of colonial conversion and progression of the malignant cell (Cox 1994).

Time scale of radiation interaction

Ionising radiation interacts with cellular systems by altering the structure, function and response of the cell to cellular products. Damage by ionising radiation affects: the cell membrane; the energy metabolism; the enzymes activities; rate of DNA synthesis; causes structural chromosomes aberrations and mutation; and influences the process of cell division. It has been shown that the cell nucleus and in particular the DNA is the primary site of damage for ionising radiation. Interaction of radiation with DNA induce a variety of molecular damage such as single strand break (SSB), double strand breaks (DSB), base damage (BD), DNA-protein cross links and others. *Molecular damage* is the result of the deposition of energy and production of ionised

* Corresponding author:

Dr. H. Nikjoo, MRC Radiation and Genome Stability Unit, Harwell, Oxfordshire, OX11 Oxford, UK. Fax: +44-1235-841200. E-mail: h.nikjoo@har.mrc.ac.uk

and excited states of the molecules - physical events, radical species and other molecular products in the environment of the DNA - chemical events. The time domain of radiation action starts with the transfer of energy from the primary particle to the molecules of the medium at times less than femto seconds (10^{-15} s). Transfer of energy to the surrounding medium initiates a chain of events depending on the magnitude of energy being transferred and electronic structure of the material of the medium. These interactions, in the forms of clusters of ionisations and excitations, set in motion one or more electrons in the surrounding molecules. These events have a random distribution and normally no two particles produce the same distribution. The energy degradation of the primary particles continue by successive interactions with the neighbouring molecules and the ejection of secondary electrons until its excess energy is completely lost and the electron becomes trapped by the electrostatic charges. The trapped electron is usually referred to as the hydrated electron (e^-_{aq}).

Hydrated electrons behave as free radicals, diffuse and interact with other atoms until captured. The creation of hydrated electrons is

regarded as the start of the chemical stage of the interaction of radiation with matter at which time the system is in thermal equilibrium. At this stage the initial energy of the primary particle and all its delta rays have been transferred to the neighbouring molecules where free radicals and excited molecules have been created. The chemistry of hydrolysis of free radicals become important in radiation biology because a large proportion of cell constituents is made up of water. Therefore the main concern of radiation chemistry is to follow the behaviour of free radicals and their subsequent interactions. A simple consequence of free radical diffusion and reactions with other molecules is the modification and amplification of existing molecular damage from the physical stage as the result of direct interactions in the target site. With the advent of fast photochemistry techniques it is now possible to get information on many of the reactions at times less than 10^{-12} s (Guaduel 1992, Tabata *et al.* 1992). Table 1 summarises the time domain of radiation effects in biological systems. The numbers in the table are approximate as duration of each stage is a function of the type of system being irradiated.

Table 1. Time domain of radiation action

Time (s)	Event
Physical stage	
10^{-18}	Energy transfer
10^{-15}	Ionising particle traverses a molecule:
10^{-14}	Ionisation
	Excitation:
	molecular vibration
	molecular dissociation
	electron thermalisation
Chemical stage	
10^{-12}	Formation of radical species & molecular product
10^{-10}	Diffusion of free radicals
10^{-8}	Free radical reactions with the solute
10^{-5}	Formation of molecular products
	Completion of chemical reactions
Biochemical stage	
1s - 1hr	Enzymatic reactions, repair processes
Biological stage	Genomic instability, aberration, mutation,
1 hr - 100 yrs	cell killing
Early effects	stem cell killing, normal-tissue damage and loss of cell
days - months	proliferation
Late effects	fibrosis, telangiectasia, skin damage, spinal cord
days - years	damage, blood vessel damage
Carcinogenesis	
many years	Appearance of tumours & secondary tumours

Chemical alterations due to direct ionisation of the molecules and free radical reactions lead to degradation of the biomolecule and induction of cross-linking, intercross-linking of the DNAs, protein etc. These and other changes to the conformation of the biomolecules may change the enzymatic activity of the cell. Table 2 provides a quantitative summary of the number of events produced by 1 Gy of radiation of different quality in a mammalian cell (Nikjoo *et al.* 1988). The differences observed in biological effects of radiations of different quality may arise not only from differences in their track structures but also from differences in physical and physiological conditions. It is noted that although energy deposited in the cell by 1 Gy of radiation produces a large number of events (apprx. 10^5 ionisations or excitations) only a fraction of these lead to induction of molecular damage. In mammalian cells, majority of single strand breaks, in the form of single nucleotide gaps, and damage to DNA bases, in the form of base products, are readily repaired (Deeble and Schuchmann 1990).

Size scale and organisation of biological targets

Figure 1 shows diagrammatic representation of the organisation of DNA in mammalian cells. Human somatic cells contain nearly 3000 Mb of DNA per haploid genome ranging from 50 to 260 Mb. The human haploid cell contains 22 pairs of chromosomes and 2 sex X and Y chromosomes, whereas *E. coli* contains only 5 Mbp of DNA. Table 3 shows comparison of some genome sizes.

DNA structure

The genome of mammalian cell contains 6 pg of DNA in a nucleus with average molecular weight of 660 for an average base pair, the diameter of a B-DNA is 2.3 nm with a base-pair width of about 0.34 nm and the number of genome per cell is 9.3×10^8 . There are 2.9×10^7 nucleosome per genome, each with diameter of 10 nm and 5nm width, assuming 190 base-pairs containing 50 nm of DNA including the linker DNA. Similarly, the

genome contains 1.9×10^6 solenoids of chromatin each of 30 nm cross section and 50 nm segment length.

Table 2. Average yield of damage in a single mammalian cell after 1 Gy of radiation.

<i>Radiation</i>	<i>Low-LET</i>	<i>High-LET</i>
Tracks in nucleus	1000	2
Ionisation in nucleus	100000	100000
Ionisation in DNA	1500	1500
Excitation in DNA	1500	1500
Base damage	10^5	10^5
DNA SSB	850	450
8-hydroxyadenine	700	-
Thymine damage	250	-
DNA DSB: initial	40	70
8 hrs	6	30
PCC Breaks: initial	6	12
8 hrs	<1	4
DNA protein cross link	150	-
Chromosome aberration	1	3
Dicentric	0.1	0.4
HPRT mutation	10^{-6}	10^{-5}
Lethal lesions	0.5	2.6
Cell inactivation	30%	85%

Although the structure of DNA was proposed in 1953 by Watson and Crick it was not until early 80's that the DNA crystal structures were solved (Dickerson and Dew 1981). The ability to make oligonucleotides of specified sequence signalled the beginning of a new era in DNA structure as, given enough material, these oligonucleotides could be crystallised and subject to X-ray crystallographic analysis. Such structures were not necessarily constrained by helical symmetry and thus for the first time it was possible to see changes in structure which might be due to the local sequence (Dickerson *et al.* 1982).

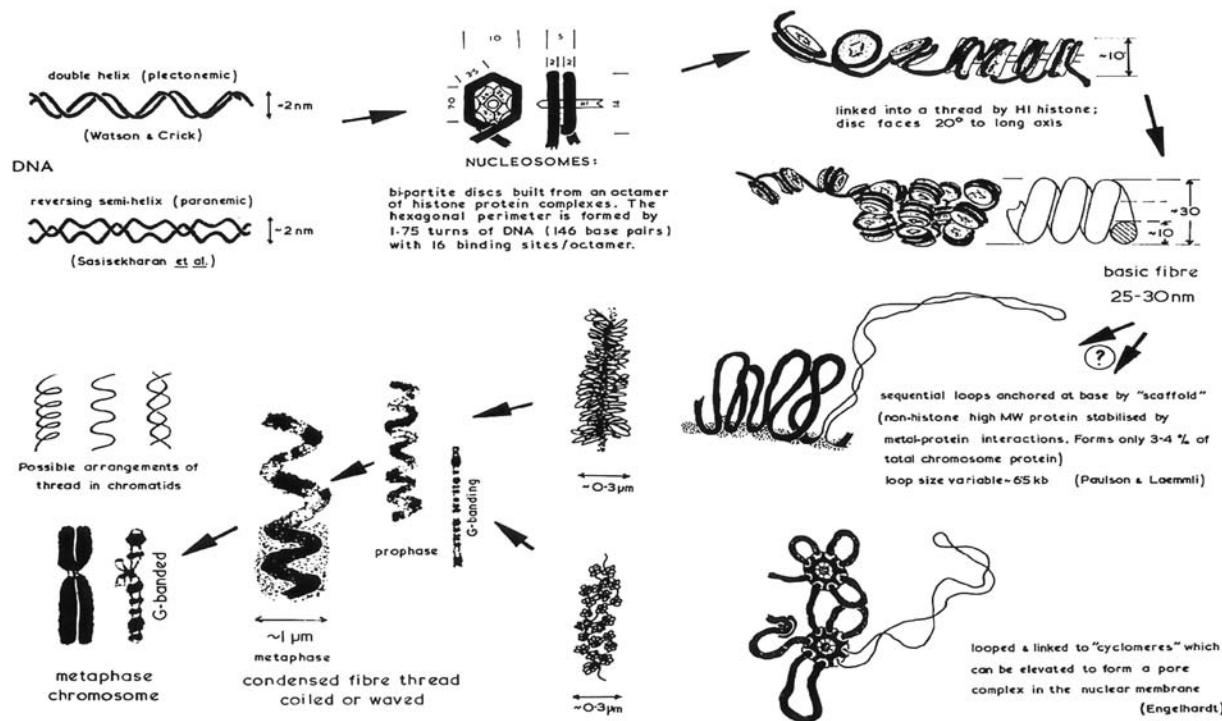


Figure 1. Construction of chromosome, (Reproduced by kind permission of J.R.K. Savage).

Table 3. Genome size of different organisms.

Genome	No. base pairs (kb)	Total length (μm)
Eukaryotes		
Human	3286,000	110,000
Drosophila	160	56,000
Yeast	13.5	4,590
Bacteria		
<i>E. coli</i>	5000	1,700
Viruses		
Fowlpox	280	93
T2, T4, T6	166	55
Phage λ	50	16
T7	40	13
ϕ X174	6.4	1.8
SV40	5.1	1.7

There are two major types of DNA conformations: A-type and B-type. Conformations belonging to both A and B families have been found in many crystal structures containing considerable volume of

aqueous solvent. A novel left-handed helix, Z-DNA, has also exists in sequences with alternating C and G bases. The advent of high-resolution, well-refined X-ray structures has led to a wealth of information about the conformations available to duplex DNA oligonucleotides. Thus, apart from the backbone torsion angles the glycosidic torsion angle and the sugar pucker, we now have to consider the detailed conformation of the bases within and between base pairs. This has lead to an agreed nomenclature as accepted methods for the calculation of such parameters as encoded in Newhelix (Dickerson et al. 1982) and CURVES (Lavery and Skelnar 1988).

The DNA fibres could exist in three major forms, as B-DNA under conditions of high humidity, as A-DNA and as a left-handed family of Z-DNA. The differences between the families occur in the way the sugar-phosphate backbone is wrapped around the helix axis, the way in

which the base-pairs are stacked and in the pucker of the furanose ring (Dickerson 1982). The A-DNA is much more compressed, it has 11 base-pairs per pitch of 0.28 nm, than the B-DNA form with 10 base-pairs per pitch of 0.34 nm. Another difference between the A and B forms is that the sugar in the B-DNA is puckered in the C (2')-endo family region, extending from O (4')-endo to C (1')-exo, resulting in a wide interphosphate separation of 0.66 nm along the chain. For the A-DNA, the sugar puckering is confined to the C (3')-endo resulting in a shorter interphosphate separation of approximately 0.6 nm. Thus, the phosphate groups in A-DNA can be bridged by water molecules as the interphosphate distances is not too large while in

B-DNA all phosphate groups are individually hydrated because the interphosphate separation is too large (Saenger 1986). These differences result in different hydration patterns around the phosphate groups, which may offer a scheme for the transition from A to B form of DNA.

Distribution of water molecules around the polar atoms of a canonical decamer B-DNA structure were obtained from quantitative analysis of the solvent interactions within hydrogen bonding distances of polar atoms of oligonucleotides using 12 B-DNA crystal structure (Umrania *et al.* 1995). Figure 2 shows a nucleotide base-pair including the first hydration shell.

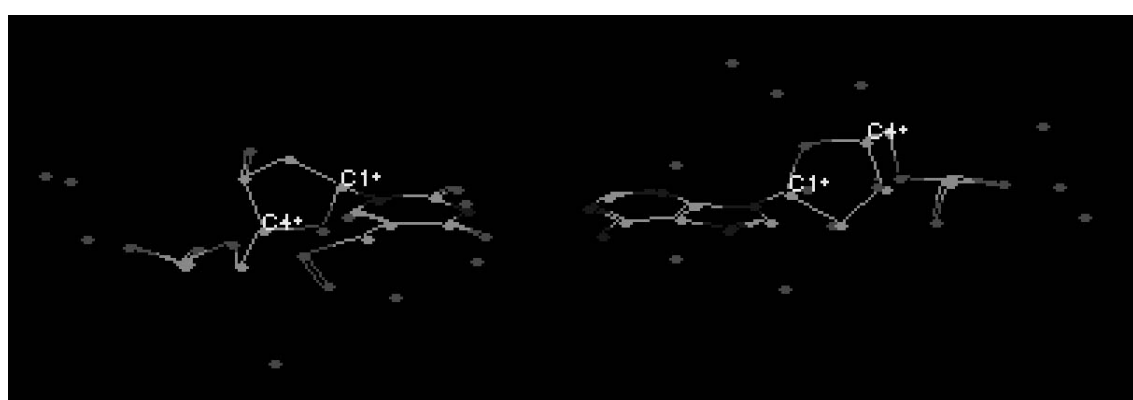


Figure 2. Nucleotide base-pair including the first hydration shell.

Track structure simulation

To date a large body of scientific literature has been generated which employ Monte Carlo track structure calculations for predicting the measurable parameters from biological experiments for understanding mechanism of damage in molecular radiation biology (Parezke *et al.* 1995, Goodhead 1994, Ward 1995). Our knowledge of spatial distributions of energy deposition in biological structures is mainly based on track structure studies in water and such data have been used in biophysical modelling of cellular effects of ionising

radiations (Holley *et al.* 1990, Nikjoo *et al.* 2001).

Broadly, track structure codes can be classified into five categories. First, target related track methods for the analysis of radiations based on a single track parameter such as LET, and ionisation yields applied to particular microscopic problems. Second, descriptions based on track segment analysis and the distinction between track entities defined as 'spur', 'blob' and 'short track'. Third, Condensed-History Monte Carlo codes for macroscopic description of dose distribution

used in radiological physics, structure analysis, accelerator beam simulation and others. Fourth, amorphous track descriptions based on average radial dose profiles around the charged particle trajectories (Cucinotta *et al.* 1999). And fifth, the full molecular interaction by interaction track structure codes with complete stochastics. Table 4 presents a list of CHMC codes which approximates the electron degradation by multiple scattering theories in combination with a small number of catastrophic events and the restricted stopping power. Most of these codes

are available commercially from the vendors for various types of platforms. Table 5 presents a list of Monte Carlo track structure codes most widely used in radiation biophysics. These codes are not in public domain and mainly used in research for understanding fundamental aspects of radiation track interactions in biological media, DNA damage evaluation and surface spectroscopy.

Table 4. Condensed history of Monte Carlo track codes in radiation research.

Code	Medium	Particle	Energy Range	Ref
EGS4	User defined	e^- , phot	10 keV - 1 GeV	a
FLUKA	User defined	e^- , e^+ , phot	1keV- PeV	b
GEANT4	User defined	HEP	keV - GeV	c
MCNP	User defined	Neutron	eV - GeV	b
PENELOPE	User defined	e^- , e^+	1keV-100MeV	b
PREGRINE	User defined	e^- , phot	Therapy beam	b

a) Nelson *et al.* 1985, b) MC2000 (2001), c) GEANT4

Table 5. Monte Carlo track codes in radiation biology.

Code	Author	Medium	Particle	Energy Range
MOCA8	Paretzke (1987)	H_2O (v, l)	e^-	10 eV - 100 keV
OREC	Turner <i>et al.</i> (1983)	H_2O (l)	e^-	10 eV - 1 MeV
			p & α	0.3 - 4 MeV/u
STBRGEN	Chatterjee&Holley (1993)	H_2O (l)	e^-	0.1 - 2 keV
			ions	0.3 - GeV
CPA100	Terrissol & Baudre (1990)	H_2O (l)	e^-	10 eV - 100 keV
DELTA	Zaider <i>et al.</i> (1983)	H_2O (v,l)	e^-	10 eV - 10 keV
			p & α	0.3 - 4 MeV/u
ETRACK	Ito <i>et al.</i> (1987)	H_2O (v)	e^-	10 eV - 10 keV
TRION	Lappa <i>et al.</i> (1993)	H_2O (v,l)	e^-	10 eV - 1MeV
			p & α	0.3 - 4 MeV/u
TRACEL	Tomita <i>et al.</i> (1997)	H_2O (v, l)	e^-	10 eV - 1 MeV
MOCA14	Wilson & Paretzke (1981)	H_2O (v)	P & α	0.3 - 4 MeV/u
PITS	Wilson & Nikjoo (1999)	H_2O (v, l)	Ions	> 0.3 MeV/u
KURBUC	Uehara & Nikjoo (1993)	H_2O (v)	e^-	10 eV - 10 MeV
LEPHIST	Uehara & Nikjoo (2001)	H_2O (v)	P	1keV - 1MeV
LEAHIST	Uehara & Nikjoo (2002)	H_2O (v)	α	1keV - 8MeV
CHEMKUR	Uehara & Nikjoo (2003)	H_2O (l)	radical	>10 ⁻¹² s
BUCK			chemistry	

v- vapour, l- liquid

Application of track structure to biophysical modelling

Energy deposition

To identify the relevant physical, chemical and biological parameters responsible for radiation effect at molecular level, commonly used parameters such as dose, fluence, LET and specific energy were found to be inadequate. Therefore track structure scoring of energy deposition in molecular volume were initiated to seek those quantities of local energy deposition that do or do not correlate with observed biological effectiveness of different radiations. In this it has become possible to set a constrain on the range and options of biophysical models of radiation action to guide experiments (Brenner *et al.* 1994). The conceptual framework of the method is to simulate the irradiation of biological experiments by generating a particle passing through a nucleus and locating the DNA hit and amount of energy deposited at the site of interaction. In this way data have been constructed on probability of energy deposition by particles of low and high LET in DNA and higher order macromolecule structures. Figure 3 shows the frequency of energy deposition in a volume similar to DNA and nucleosome.

DNA damage

There has long been indications that the biological consequences of ionising radiations are determined primarily by their properties of clustering of ionisations at the level of DNA duplex (Goodhead 1994), rather than at the level of micrometers as was the focus of much microdosimetry during the 70's and 80's. With the derivation of a systematic database of frequencies of energy deposition in small volumes, of dimensions 1nm upward, for a wide variety of radiations, it became possible to seek the regions which correlate with particular biological effects. This approach makes *no a priori* assumptions about the nature of the biological targets. The first such application of track scoring was for X-rays of various energies

indicating that the critical properties lay in the region greater than 100 eV of energy deposition, clustered within a distance of about 3 nm (Goodhead And Brenner 1983). In the same manner, the dominant feature associated with the high-LET effects was found to correspond to a larger class cluster of energy greater than 340 eV in nucleosome size targets. Subsequent comparisons have shown that the smaller clusters correlate well with measured yields of DNA double strand breaks for photons and alpha particles (Goodhead and Nikjoo 1989).

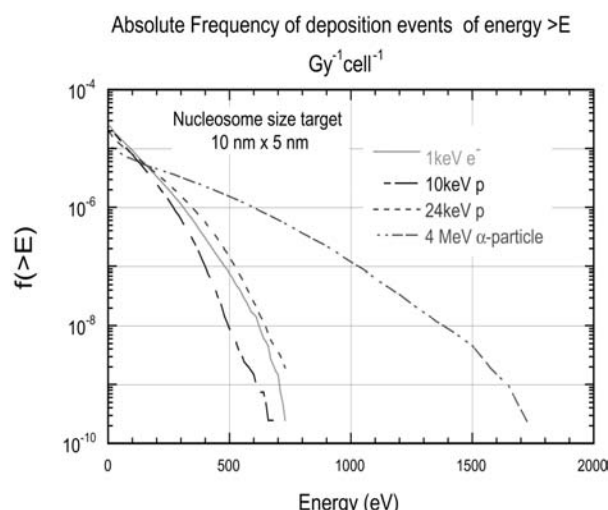


Figure 3. Frequency distribution of energy deposition in a target corresponding in size to a volume of dimensions similar to a nucleosome 10nm diameter by 5nm height in water irradiated with monoenergetic electrons with initial energy 1keV, 4 MeV alpha-particles, 10 keV and 24 keV protons. The left ordinate gives the absolute frequency $f(>E)$ of deposition events greater than the energy E deposited in the target volume when randomly placed in the cell nucleus and uniformly irradiated with 1 Gy of the given radiation.

These studies have indicated that the predominant features of radiations can be usefully considered in terms of four classes of initial clustered damage of increasing severity summarised in table 6. (Charlton *et al.* 1992)

Table 6. Classification of clusters according to energy deposited in the target.

Class	Initial physical damage	Energy deposited in the target	Possible target size	Frequency of occurrence (Cell ⁻¹ Gy ⁻¹)	Comment
1	Sparse	Few tens of eV within ~2nm	DNA segment	~103	Little biological relevance
2	Moderate clusters	~100 eV within ~2nm	DNA segment	~20-100	Characteristic of low-LET; reparable
3	Large clusters	~400 eV within 5-10 nm	Nucleosome	~4-100	Characteristic of low-LET; unreparable
4	Very large clusters	~800 eV within 5-10 nm	Nucleosome	~0-30	Unique to high-LET; unreparable; special relevance?

It has been suggested that class 1 damage is predominantly single strand breaks and simple type; class 2 is mainly of double strand type breakage; class 3 is of more complex double strand breaks; and class 4 is complex type of double strand break damage.

An alternative way of using the detail provided by the Monte Carlo track structure approach is to examine the way in which energy is deposited by ionisations and excitations at sugar-phosphate moiety and the bases and relating it to an initial biological lesion which can be measured experimentally. Various parameters have been used to achieve such a relationship including 'ionisation' and a 'quantity of energy' to induce a single strand break or double strand break by various authors (Nikjoo *et al.* 1996, 1997, Charlton *et al.* 1989, Charlton & Humm 1988). In my work I have employed an amount of or threshold energy E_{th} deposited by a single track at a sugar-phosphate site for induction of a single strand break which is derived from a knowledge-based model (52-54). In this work the threshold energy for induction of a single strand break was set at $E_{th}=17.5$ eV. Using this criterion for the induction of a ssb the energy deposition patterns from charged particle tracks can be converted to distributions of single strand breaks along the hit section of the DNA. When two single strand

breaks on opposite strands were separated by a distance less than ten base-pair it is assumed that a double strand break is produced. Figure 4 shows the relationship between the energy deposited and the number of single strand breaks and the probability of induction of a double strand break in DNA. The data shows a universal curve for all radiations of low and high LET independent of the type of radiation. This is expected as complexity of damage depends on patterns of energy deposition rather than the source of radiation. (Nikjoo *et al.* 1997).

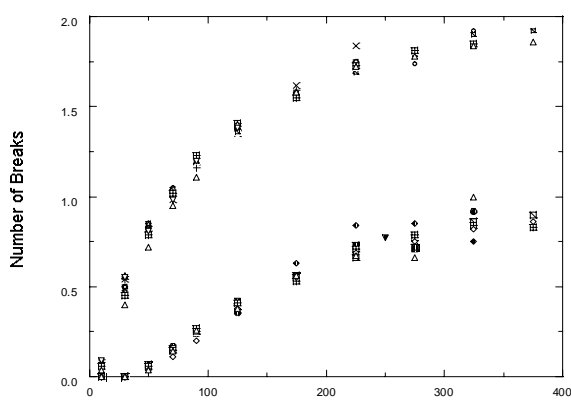


Figure 4. The relationship between energy deposited in the DNA and the numbers of single or double strand breaks.

The threshold energy concept deals with the direct interaction of track with the target. Radical species such e^-_{aq} , $\cdot H$ and $\cdot OH$ are also produced in the bulk water associated with DNA. Among these hydroxyl radicals are the most damaging agent and their movement are assumed to be diffusion controlled. Reaction of OH radicals with sugar produce sugar radicals. Not all sugar radicals lead to strand break. In general, about 20% of sugar radicals are converted to strand break. Therefore, in the cellular environment a probability of 0.13 for the induction of a single strand break by hydroxyl radical can be assumed. This is implicitly composed of 0.2 probability of an OH reacting with sugar and 0.8 with the nucleobases. Of those radicals reacting with the sugar-phosphate there is a probability of 0.65 to cause a strand break. Hydrated electrons and H radicals mainly produce base radicals (Nikjoo *et al.* 1997, 2001).

New phenomena in radiation biology

The dose-response curve for all solid cancers based on atomic bomb survivor data indicates a linear form down to doses as low as 50 mSv. However, risk estimates for radiation-induced oncogenesis at very low doses (<50mSv), a region where direct experimental observations are not available, are usually extrapolated from high doses of ionising radiation using a linear non-threshold model (ICRP-60, 1990). The validity of this approach is still the subject of investigation and discussion (NCRP-136, 2001). There are a number of factors affecting the shape of the dose-response curve at low doses of irradiation, including low-dose-hyper-radiosensitivity (Joiner, 1994), adaptive-dose-response (Azzam *et al.* 1994), genomic-instability (Kadhim *et al.* 1992) and more recently bystander effect (Mothersill and Seymour 1997). These phenomena are considered to be of significant importance in influencing the shape of the dose-response curve at low dose and dose-rate exposure to ionising radiation.

Genomic instability

In 1992 Kadhim and colleagues reported the occurrence of non-clonal aberrations in bone marrow cells in culture after traversals of on average 0.5, 1 and 2 alpha-particles assuming Poisson distribution of tracks through the cells. For an average of 1 alpha particle per cell, on average there is a probability of 0.63 of cells receive one or more traversal and 0.37 no traversal. As alpha particles are a radiation of high-LET and low penetration, produce a tracks with high density interactions (ionizations and excitations), most cells traversed by an alpha particles do not survive. The probability of survival after an alpha-particle traversal is less than 0.2. When the surviving cells were grown as separate colonies for several generations and scored for chromosome aberrations, some 50% of the colonies exhibited non-clonal abnormalities. These results were interpreted as radiation effects could arise, *de novo*, several generations after the damage inflicted. This observation of delayed response was termed *radiation-induced genomic instability* (RIGI). A recent publication by Lorimore and Wright (2002) provides a review of the genomic studies in haemopoietic systems.

Bystander effect

The bystander phenomenon deals with biological effects in cells not directly hit by radiation. The effect has been observed for a variety of biological endpoints such as cell survival (Mothersill and Seymour, 1997, 1998), mutation (Hei *et al.* 1997, Wu *et al.* 1999), sister chromatid exchange (Deshpande *et al.* 1996), cell transformation (Sawant *et al.* 2001), micronuclei and apoptosis (Prise *et al.* 1998), gene expression (Azzam *et al.* 1998) and radiation genomic-instability (Lorimore *et al.* 1998, Watson. 2000, Seymour and Mothersill, 2000). Direct experimental evidence for bystander effect has emerged from a number of laboratories (Mothersill and Seymour, 1997, 1998, Sigg *et al.* 1997, Lorimore *et al.* 1998). It was discovered that medium from irradiated mammalian cells is able to induce early events in

the apoptotic cascade in cells of the same line never exposed to radiation (Lyng *et al.* 2001, 2002).

Recent experiments involving α -particle micro-beams have demonstrated the bystander effect for cell killing and oncogenic transformation in C3H T10 1/2 cells (Sawant *et al.* 2001, Miller *et al.* 1999). These precise micro-beam experiments present an ideal opportunity for careful qualitative analysis of the role and importance of the bystander effect in the radiation response observed at low doses. In this paper a theoretical model has been constructed to study time-dependent patterns of bystander phenomenon based on diffusion type communication between cells.

The theoretical development in this topic has been rather slow. Recent papers published include those by Brenner *et al.* (2001), Little and Wakeford (2001), Brenner and Sachs (2002), Nikjoo and Khvostunov (2003).

Adaptive response

All living organisms, bacteria to humans, react to environmental stress as part of their defence mechanism. When cells are exposed to very low level doses of a toxic agent, such as carcinogens and radiation, cells become less susceptible to damage when exposed to subsequent toxic dose of the same or other agents. This behaviour has been termed *adaptive response*. The first observation of adaptive response was reported by Samson and Cairns (1977) in E.Coli. Radiation induced adaptive response was originally observed in chromosomal aberrations in human lymphocytes (Olivieri *et al.* 1984). When cells were cultured with thymidine, acting as a source of low level chronic radiation, and then exposed to X-rays, the yield of chromatid aberration was less than the sum of the yields of aberrations induced by thymidine and X-rays alone. Adaptive response has been observed for variety of biological end points including chromosome aberrations, gene mutations and cell killing (Cai 1999). Adaptive response has been observed at doses less than 20 cGy. The mechanism underlying adaptive

response has not yet been understood well. It has been proposed that at low doses radiation could trigger molecular processes which enhance the DNA repair ability and the molecular antioxidant activity (Wojcik and Streffler 1994).

Summary

This short review paper presented a brief summary of an approach to biophysical modelling as a first step towards mechanistic interpretation and prediction of radiation effect that can be compared with experiments. Data on the three stages of the modelling and calculations were presented including the transport of charged particle track, biological target structure and pathway to induction of strand breaks.

Charged particle transport and track structure simulation is now a well established tool in biophysical modelling and many such codes are available to the researchers around the world as listed in table 2. Similarly, simulation of atomistic structures of DNA in various forms can be made by codes which are available commercially. However, the data presented on the primary hydration shell is unique and the first to provide full information on the spatial coordinates of the distributions around a canonical decamer B-DNA. The hydration data shows that water interactions around the bases occur mainly with the polar atoms of the major and minor grooves. In sugar the interactions appears around the O(4') and for the phosphate group clustering of solvent appears around the O1P and O2P atoms. The distribution of water in the first hydration shell is structured and fulfils the stereochemical requirements for hydrogen bonding for polar atoms.

The Pathway to DNA damage is a highly complex subject as physical and physiological conditions affects the response of the cell to damage by ionising radiation. The method adopted in my work is based on knowledge deduced from relevant biological experiment. In the first instance, it is assumed that the observed biological lesions are mainly mediated by the induction of double strand breaks. It is assumed

that a double strand break is composed of two single strand breaks on opposite strand placed near each other and are induced by a single particle traversal. A quantity of 17.5 eV is used for the induction of a single strand break by direct interaction and a probability of 0.13 for the induction of single strand break when an OH radical reacts with a sugar-phosphate moiety. Calculations show that majority of damaged sites are simple, consisting of a single strand break or base damage but a substantial proportion, more than 20%, of the damages sites contain additional damage, and that the contribution of hydroxyl radicals to the total yield of strand breakage is a function of activation probability.

It is observed that for low LET radiations ~90% of total energy deposited in DNA are due to energy depositions events less than 60 eV but the largest dsb yield is due to energy depositions in the range 100-150 eV. Similarly, although the initial yield of strand breakage is nearly unity for all radiations, the complexity of strand breaks increase with increase in LET of the particle.

REFERENCES

Azzam E.I., Toledo S.M., Gooding T., Little J.B. (1998). Intercellular communication is involved in the bystander regulation of gene expression in human cells exposed to very low fluences of alpha particles. *Radiat. Res.*, **150**: 497-504.

Azzam E.I., Raaphorst G.P., Mitchel R.E.J. (1994). Radiation-induced adaptive response for protection against micronucleus formation and neoplastic transformation in C3H 10T 1/2 mouse embryo cells. *Radiat. Res.*, **138**: S28-S31.

Brenner D.J., Little J.B., Sachs R.K. (2001). The bystander effect in radiation oncogenesis: II. A quantitative model. *Radiat. Res.*, **155**: 402-408.

Brenner D.J. and Sachs R.K. (2002). Do low dose-rate bystander effects influence domestic radon risks? *Int. J. Radiat. Biol.*, **78**: 593-604.

Brenner D.J., Ward J.F., Sachs R.K. (1994). Track structure, chromosome geometry and chromosome aberrations. Varma M.N., Catterjee A. (eds.), Computational Approaches in Molecular Radiation Biology, Monte Carlo Methods. *Plenum Press New York*. 93-113.

Cai L. and Wang P. (1995). Induction of a cytogenetic adaptive response in germ cells of irradiated mice with very low-dose rate of chronic gamma irradiation and its biological influence of radiation-induced DNA or chromosomal damage and cell killing in their male offspring. *Mutagenesis*, **10**: 95-100.

Charlton D.E., Nikjoo H., Humm J.L. (1989). Calculation of initial yields of single and double strand breaks in cell nuclei from electrons, protons and alpha particles. *Int. J. Radiat. Biol.*, **56**: 1-19.

Charlton D.E. and Humm J.L. (1988). A method of calculating initial DNA strand breakage following the decay of incorporated ¹²⁵I. *Int. J. Radiat. Biol.*, **53**: 353-365.

Charlton D.E., Nikjoo H., Goodhead D.T. (1992). Energy deposition in sub-microscopic volumes. Dewey W.C., Edington M., Fry R.J., Hall E.J. and Whitmore G.F. Radiation Research: A twentieth-century perspective. Vol. II. Congress Proceedings. San Diego, Academic Press, 421-426.

Chatterjee A. and Holley W. (1993). Computer simulation of initial events in the biochemical mechanisms of DNA damage. *Adv. Radiat. Biol.*, **17**: 181-226.

Cox R. (1994). Molecular mechanisms of radiation oncogenesis. *Int. J. Radiat. Biol.*, **65**: 57-64.

Cucinotta F.A., Nikjoo H., Goodhead D.T. (1999). Applications of amorphous track models in radiation biology. *Radiat. Environ. Biophys.*, **38**: 81-92.

Deshpande A., Goodwin E.H., Bailey S.M., Marrone B.L., Lehnert B.E. (1996). Alpha-particle-induced sister chromatid exchange in normal human lung fibroblasts: Evidence for an extracellular target. *Radiat. Res.*, **145**: 260-267.

Deeble D.J., Schuchmann M.N., Steenken S., Von Sontag C. (1990). Direct evidence for the formation of thymine radical cations from the reaction of SO₄[·] with thymine derivatives - A Pulse-radiolysis study with optical and conductance detection. *J. Phys. Chem.*, **94**: 8186-8192.

Dickerson R.E., Drew H.E., Conner B.N., Wing R.M., Fratini A.V., Kopla M.L. (1982). Anatomy of A-, B- and Z-DNA. *Science*, **216**: 475-485.

Dickerson R.E. and Drew H.R. (1981). Structure of a B-DNA dodecamer $\ddot{\text{U}}$ Influence of base sequence on helix structure. *J. Mol. Biol.*, **149**: 761-786.

GEANT4 Collaboration: GEANT4: AN Object-Oriented Toolkit for Simulation in HEP, CERN/LHCC 98-44; see also the web site: <http://www.cern.ch/geant4>

Goodhead D.T. (1994). Initial events in the cellular effects of ionising radiations: clustered damage in DNA. *Int. J. Radiat. Biol.*, **65**: 7-17.

Goodhead D.T. and Brenner D.J. (1983). Estimation of a single property of low LET radiations which correlates with biological effectiveness. *Phys. Med. Biol.*, **28**: 485-492.

Goodhead D.T. and Nikjoo H. (1989). Track structure analysis of ultrasoft X-rays compared to high- and low-LET radiations. *Int. J. Radiat. Biol.*, **55**: 513-529.

Goodhead D.T. (1987). Relationship of microdosimetric techniques to applications in biological systems. The Dosimetry of Ionizing Radiation. In: Kase K.R., Bjarngard B.E., and Attix H. (eds.), *Academic Press, Orlando*, **1**: 1-89.

Gauduel Y. (1992). Symposium: Early Radiation Chemistry: Femtoseconds to Nanoseconds. Concept Design of Electron Femtosecond Pulse Radiolysis, Radiation Research: A Twentieth-Century Perspective, Volume $\ddot{\text{U}}$ F Congress Proceedings, Dewey W.C., Edington M., Fry R.J.M., Hall E.J. and Whitmore G.F. (eds.), *Academic Press*, 50.

Hei T.K., Wu L.J., Liu S.X., Vannias D., Waldren A., Randers-Peterson G. (1997). Mutagenic effects of a single and an exact number of alpha-particles in mammalian cells. *Proc. Natl. Acad. Sci. USA*, **94**: 3765-3770.

Holley W.R., Chatterjee A., Magee J.L. (1990). Production of DNA strand breaks by direct effects of heavy charged particles. *Radiat. Res.*, **121**: 161-168.

ICRP (1990). Recommendations of the International Commission on Radiological Protection. *Publication 60, Annals of the ICRP*, **21**, No. 1-3, Pergamon Press, Oxford.

Ito A. (1987). Calculation of double strand breaks probability of DNA for low LET radiations based on track structure analysis. Nuclear and atomic Data for Radiotherapy and Related Radiobiology, IAEA, Vienna.

Joiner M.C. (1994). Induced radioresistance: An overview and historical perspective. *Int. J. Radiat. Biol.*, **65**: 79-84.

Kadhim M.A., Macdonald D.A., Goodhead D.T., Lorimore S.A., Marsden S.J., Wright E.G. (1992). Transmission of chromosomal instability after plutonium alpha-particle irradiation. *Nature* **355**, 738-740.

Lappa A.V., Bigildeev E.A., Burmistrov D.S., Vasilyev O.N. (1993). Trion code for radiation action calculations and its application in microdosimetry and radiobiology. *Radiat. Environ. Biophys.*, **32**: 1-19.

Lavery R. and Sklenar H. (1988). The definition of generalised helicoidal parameters and of axis curvature for irregular nucleic acids. *J. Biomol. Struct. Dynam.*, **6**: 63-91.

Little M.P. and Wakeford R. (2001). The bystander effect in C3H10T1/2 cells and radon-induced lung cancer. *Radiat. Res.*, **156**: 695-699.

Lorimore S.A. and Wright E.G. (2002). Radiation-induced genomic instability and bystander effects: related inflammatory-type responses to radiation-induced stress and injury. A review. *Int. J. Radiat. Biol.*, **79**: 27-34.

Lorimore S.A., Kadhim M.A., Pocock D.A., Papworth D., Stevens D.L., Goodhead D.T., Wright E.G. (1998). Chromosomal instability in the descendants of unirradiated surviving cells after alpha-particle irradiation. *Proc. Natl. Acad. Sci. USA*, **95**: 5730-5733.

Lyng F.M., Seymour C.B., Mothersill C. (2001). Oxidative stress in cells exposed to low levels of ionising. *Radiat. Biochem. Soc.*, **T. 29: Part 2**, 350-353.

Lyng F.M., Seymour C.B., Mothersill C. (2002). Initiation of apoptosis in cells exposed to medium from the progeny of irradiated cells: A possible mechanism for bystander-induced genomic instability. *Radiat. Res.*, **157**: 365-370.

MC2000 (2001). Kling A., Barao F., Nakagawa M., Tavora L., Vaz P. (eds.) Advanced Monte Carlo for Radiation Physics, Particle Transport Simulation and Applications. *Springer-Verlag Berlin*.

Miller R.C., Randers-Pehrson G., Geard C.R., Hall E.J., Brenner D.J. (1999). The oncogenic transforming potential of the passage of single α -particles through mammalian cell nuclei. *Proc. Natl. Acad. Sci.*, **96**: 19-22.

Mothersill C. and Seymour C. (1997). Medium from irradiated human epithelial cells but not human

fibroblasts reduces the clonogenic survival of unirradiated cells. *Int. J. Radiat. Biol.*, **71**:421-427.

Mothersill C. and Seymour C. (1998). Cell-cell contact during gamma irradiation is not required to induce a Bystander effect in normal human keranocytes: evidence for release during irradiation of a signal controlling survival into the medium. *Radiat. Res.*, **149**: 256-262.

Mothersill C. and Seymour C. (2001). Radiation-induced bystander effects: past history and future directions. A review. *Radiat. Res.*, **155**: 759-767.

NCRP (2001). Report No. 136. Evaluation of the linear-non-threshold dose-response model for ionizing radiation. *National Council on Radiation Protection and Measurements*. Bethesda, Maryland 30814-5916.

Nelson W.R., Hirayama H., Rogers D.W. (1985). The EGS4 Code System. *SLAC-Report-265*.

Nikjoo H., O'Neill P. Goodhead D.T., Terrissol M. (1997). Computational modelling of low-energy electron-induced DNA damage by early physical and chemical events. *Int. J. Radiat. Biol.*, **71**: 467-483.

Nikjoo H., Uehara S., Wilson W.E., Hoshi M., Goodhead D.T. (1998). Track structure in radiation biology: theory and applications. *Int. J. Radiat. Biol.*, **73**: 355-364.

Nikjoo H. and Khvostunov I.K. (2003). A Biophysical Model of Radiation Induced Bystander Effect. *Int. J. Radiat. Biol.*, **1**: 43-52.

Nikjoo H., Martin R.F., Charlton D.E., Terrissol M., Kandaiya S., Labachevski P. (1996). Modelling of Auger-induced DNA damage by incorporated ¹²⁵I. *Acta Oncologica*, **35**: 849-856.

Olivieri G., Bodycote J., Wolff S. (1984). Adaptive response of human lymphocytes to low concentrations of radioactive thymidine. *Science* **233**: 594-597

Paretzke H.G., Goodhead D.T., Kaplan I.G., Terrissol M. (1995). Atomic & Molecular data for radiotherapy and radiation research. *IAEA, Vienna, Tecdoc-799*, 633-721.

Paretzke H.G. (1987). Radiation track structure theory. *Kinetics of Nonhomogeneous Processes*, Freeman G.R. (ed.), 89-170. *John Wiley and Sons, New York*.

Prise K.M., Belyakov O.V., Folkard M., Michael B.D. (1998). Studies of bystander effects in human fibroblasts using a charged particle microbeam. *Int. J. Radiat. Biol.*, **74**: 793-798.

Saenger W. (1986). *Principles of Nucleic Acid Structure*. Springer Verlag.

Samson L. and Cairns J. (1977). A new pathway for DNA repair in *Escherichia coli*. *Nature*, **267**: 281-283.

Sawant S.G., Randers-Pehrson G., Geard C.R., Brenner D.J., Hall E.J. (2001). The bystander effect in radiation oncogenesis: I. Transformation in C3H 10T ½ cells in vitro can be initiated in the unirradiated neighbours of irradiated cells. *Radiat. Res.*, **155**: 397-401.

Seymour C.B. and Mothersill C. (2000). Relative contribution of bystander and targeted cell killing to the low-dose region of the radiation dose response curve. *Radiat. Res.*, **153**: 508-511.

Sigg M., Crompton N.E.A., Burkrat W. (1997). Enhanced neoplastic transformation in an inhomogeneous radiation field: an effect of the presence of heavily damaged cells. *Radiat. Res.*, **148**: 543-547.

Tabata Y. and Kobayashi H. (1992). Symposium: Early Radiation Chemistry: Femtoseconds to Nanoseconds, Concept Design of Electron Femtosecond Pulse Radiolysis, Radiation Research: A Twentieth-Century Perspective, Volume [‡]U• F Congress Proceedings, Dewey W.C., Edington M., Fry R.J.M., Hall E.J., Whitmore G.F. (eds.), Academic Press, 58.

Terrissol M. and Beaudre A. (1990). Simulation of space and time evolution of radiolytic species induced by electron in water. *Radiat. Protec. Dosim.*, **31**: 171-175.

Tomita H., Kai M., Kusama T., Ito A. (1997). Monte Carlo simulation of physicochemical processes of liquid water radiolysis - The effects of dissolved oxygen and OH scavenger. *Radiat. Environ. Biophys.*, **36**: 105-116.

Turner J.E., Magee J.L., Wright H.A., Chatterjee A., Hamm R.N., Ritchie R.H. (1983). Physical and chemical development of electron tracks in liquid water. *Radiat. Res.*, **96**: 437-449.

Uehara S., Nikjoo H., Goodhead D.T. (1993). Cross sections for water vapour for Monte Carlo track structure code from 10 eV to 10 MeV region. *Phys. Med. Biol.*, **38**: 1841-1858.

Uehara S. and Nikjoo H. (2003). Monte Carlo simulation of water radiolysis by electrons and ions. (unpublished).

Uehara S., Toburen L.H., Nikjoo H. (2001). Development of a Monte Carlo track structure code for low-energy protons in water. *Int. J.*

Radiat. Biol., **77**: 138-154.

Umrania Y., Nikjoo H., Goodfellow J.M. (1995). A knowledge-based model of DNA hydration. *Int. J. Radiat. Biol.*, **67**:145-152.

UNSCEAR (1993). Sources and effects of ionizing radiation. United Nations Scientific Committee on the Effects of Atomic Radiation. Report to the General Assembly. Annex F: Influence of dose and dose rate on stochastic effects of radiation.

Vogelstein B. and Kinzler K.W. (1998). The genetic basis of human cancer. *McGrow-Hill, New York*.

Ward J.F. (1995). Radiation mutagenesis: the initial DNA lesions responsible. *Radiat. Res.*, **142**: 362-368.

Watson J.D. and Crick F.H.C. (1953). Molecular Structure of Nucleic Acids. *Nature*, **171**: 737-738.

Watson G.E., Lorimore S.A., Macdonald D.A, Wright E.G. (2000). Chromosomal instability in unirradiated cells induced *in vivo* by a bystander effect of ionizing radiation. *Cancer Res.*, **60**: 5608-5611.

Wilson W.E. and Nikjoo H. (1999). A Monte Carlo code for positive ion track simulation. *Radiat. Environ. Biophys.*, **38**: 97-104

Wilson W.E., Miller J.H., Nikjoo H. (1994). PITS - A code system for Positive Ion Track Structure. Computational Approaches in Molecular Radiation Biology, Varma M.N. and Chatterjee A. (eds.). *Plenum Press, New York*. 137-153.

Wilson W.E. and Paretzke H.G. (1981). Calculation of distribution of energy imparted and ionisations by fast protons in nanometer sites. *Radiat. Res.*, **81**: 521-537.

Wojcik A. and Strelffer C. (1994). Adaptive response to ionizing radiation in mammalian cells: a review. *Biol. Zent. bl.*, **113**: 417-434.

Zaider M., Brenner D.J., Wilson W.E. (1983). The applications of track calculations to Radiobiology 1. Monte Carlo simulation of proton tracks. *Radiat. Res.*, **95**: 231-247.